Proc. Natl. Acad. Sci. USA
Vol. 93, pp. 6770–6774, June 1996
Medical Sciences

Nitric oxide synthase generates superoxide and nitric oxide in arginine-depleted cells leading to peroxynitrite-mediated cellular injury

(free radicals/electron paramagnetic resonance/spin trapping/nitrotyrosine)

YONG XIA*, VALINA L. DAWSON†‡, TED M. DAWSON†‡, SOLOMON H. SNYDER†, AND JAY L. ZWEIER*§

*Molecular and Cellular Biophysics Laboratories, Department of Medicine, Division of Cardiology and the Electron Paramagnetic Resonance Center, †Departments of Neuroscience, Pharmacology and Molecular Sciences, and Psychiatry and Behavioral Sciences, and ‡Department of Neurology, The Johns Hopkins Medical Institutions, Johns Hopkins Bayview Medical Center, Baltimore, MD 21224

Contributed by Solomon H. Snyder, March 13, 1996

ABSTRACT **Besides synthesizing nitric oxide (NO), purified neuronal NO synthase (nNOS) can produce superoxide ($^{\cdot}O_2^-$) at lower L-Arg concentrations. By using electron paramagnetic resonance spin-trapping techniques, we monitored NO and $^{\cdot}O_2^-$ formation in nNOS-transfected human kidney 293 cells. In control transfected cells, the Ca^{2+} ionophore A23187 triggered NO generation but no $^{\cdot}O_2^-$ was seen. With cells in L-Arg-free medium, we observed $^{\cdot}O_2^-$ formation that increased as the cytosolic L-Arg levels decreased, while NO generation declined. $^{\cdot}O_2^-$ formation was virtually abolished by the specific NOS blocker, *N*-nitro-L-arginine methyl ester (L-NAME). Nitrotyrosine, a specific nitration product of peroxynitrite, accumulated in L-Arg-depleted cells but not in control cells. Activation by A23187 was cytotoxic to L-Arg-depleted, but not to control cells, with marked lactate dehydrogenase release. The cytotoxicity was largely prevented by either superoxide dismutase or L-NAME. Thus, with reduced L-Arg availability NOS elicits cytotoxicity by generating $^{\cdot}O_2^-$ and NO that interact to form the potent oxidant peroxynitrite. Regulating arginine levels may provide a therapeutic approach to disorders involving $^{\cdot}O_2^-$/NO-mediated cellular injury.**

Nitric oxide (NO), a gaseous free radical, regulates vascular tone, platelet aggregation, leukocyte adhesion, synaptic transmission and cytostatic/cytotoxic actions of macrophages (1, 2). NO arises from the guanidino group of L-Arg in an NADPH-dependent reaction catalyzed by a family of NO synthases (NOSs) (3). Three distinct isoforms of NOS, derived from separate genes, are neuronal NOS (nNOS, type I), inducible NOS (type II), and endothelial NOS (type III) (4, 5). The three isoforms are similar in structure and function, utilizing L-Arg, oxygen, and NADPH as substrates and requiring FAD, FMN, calmodulin, and tetrahydrobiopterin as cofactors (6). NOS is a cytochrome P450 reductase-like hemoprotein containing FAD, FMN, NADPH, calmodulin, and ferroprotoporphyrin IX (heme) binding sites (7). The catalytic mechanism of NOS involves flavin-mediated electron transport from NADPH to the terminal heme, where oxygen is bound and incorporated into NO and citrulline (8, 9).

Besides synthesizing NO, purified porcine nNOS generates hydrogen peroxide (H_2O_2) at low concentrations of L-Arg (10, 11). Purified rat nNOS produces superoxide ($^{\cdot}O_2^-$) in an NADPH and Ca^{2+}/calmodulin-dependent manner (12). Questions not yet answered include (*i*) whether NOS-mediated $^{\cdot}O_2^-$ generation occurs in intact cells, (*ii*) how cytosolic NOS is regulated to produce either NO or $^{\cdot}O_2^-$, and (*iii*) whether in intact cells NO and $^{\cdot}O_2^-$ generated by NOS combine to form the cytotoxic oxidant peroxynitrite ($ONOO^-$). Furthermore, the biological significance of the $^{\cdot}O_2^-$ generated by NOS has not been established. In the present study, we directly measure and characterize the formation of both NO and $^{\cdot}O_2^-$ in neuronal constitutive NOS-transfected human kidney 293 cells by using electron paramagnetic resonance (EPR) spin-trapping techniques. The effects of intracellular L-Arg depletion on the NOS-catalyzed generation of NO and $^{\cdot}O_2^-$ are determined as well as the role of these radicals in the process of cellular injury.

MATERIALS AND METHODS

Materials. The Ca^{2+} ionophore A23187, *N*-nitro-L-arginine methyl ester (L-NAME), superoxide dismutase (SOD), and other chemicals, or solvents were purchased from Sigma, unless noted otherwise. Cell culture materials were obtained from GIBCO/BRL. *N*-Methyl-D-glucamine dithiocarbamate (MGD) was synthesized as described (13). The *N*-methyl-D-glucamine and carbon disulfide required for MGD synthesis were purchased from Aldrich and 5,5-dimethyl-1-pyrroline-*N*-oxide (DMPO) was from Oklahoma Medical Research Foundation (Oklahoma City, OK).

Cell Culture and Cytosolic L-Arg Depletion. Human embryonic kidney 293 cells (HEK 293) were obtained from American Type Culture Collection and cultured in minimum essential medium (MEM) with 10% heat-inactivated fetal calf serum (GIBCO/BRL) at 37°C in a 5% CO_2/95% air humidified incubator. A stable rat nNOS-transfected cell line was established by cotransfection of pCIS-NOS with pRSV-NEO (Genentech) into HEK 293 cells as reported (7). These NOS-transfected 293 cells were maintained under selective pressure by treating the cells with Geneticin (500 μg/ml) at every sixth passage. To deplete intracellular L-Arg, the cells were cultured in MEM until 80–90% confluent and then the medium was replaced by Select-Amine MEM (GIBCO/BRL) containing all other amino acids except L-Arg. Cultured cells were washed three times with Dulbecco's phosphate-buffered saline (pH 7.4) containing 0.9 mM $CaCl_2$ and 5.5 mM glucose (PBS, GIBCO/BRL) and harvested in PBS by using a rubber scraper.

HPLC Measurement of Intracellular Amino Acids. Cells were harvested as described above. Intracellular free amino acids were extracted using ice-cold 0.3 M perchloric acid, and the extract was neutralized by 3 M $KHCO_3$. The protein and cellular debris in the preparations were pelleted by centrifugation (10,000 × *g* for 20 min) at 4°C, and the supernatant was recovered for HPLC analysis. The samples were then dried under vacuum and derivatized by a reagent containing methanol, triethylamine, water, and phenyl isothiocyanate at a

The publication costs of this article were defrayed in part by page charge payment. This article must therefore be hereby marked "*advertisement*" in accordance with 18 U.S.C. §1734 solely to indicate this fact.

Abbreviations: NOS, NO synthase; nNOS, neuronal NOS; MGD, *N*-methyl-D-glucamine dithiocarbamate; DMPO, 5,5-dimethyl-1-pyrroline-*N*-oxide; L-NAME, *N*-nitro-L-arginine methyl ester; SOD, superoxide dismutase; LDH, lactate dehydrogenase.

§To whom reprint requests should be addressed.

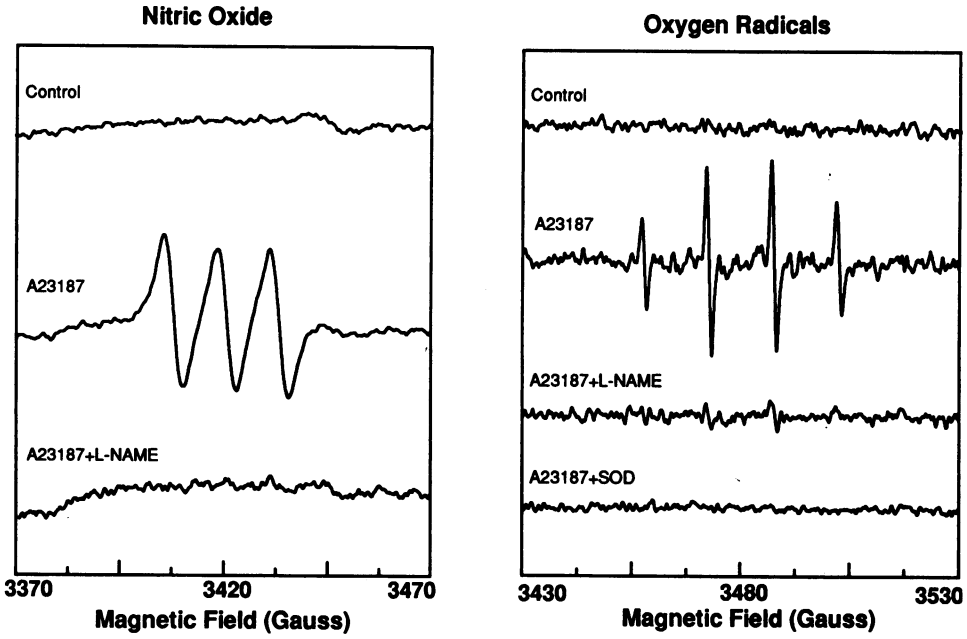

FIG. 1. Activation with calcium ionophore stimulates NO and oxygen radical formation. Measurements were performed on 5 × 10^6 cells per ml in PBS at room temperature. (*Left*) EPR spectra of NO trapping using Fe–MGD. Spectra were recorded with a microwave frequency of 9.77 GHz by using 20 mW of microwave power and a 3.2-G modulation amplitude. Spectra: control, spectrum obtained from cells in the absence of A23187; A23187, cells after addition of 1 μM A23187; A23187 + L-NAME, cells cultured with 1 μM A23187 and 1 mM L-NAME. (*Right*) EPR spectra of oxygen radical generation from cells subjected to L-Arg depletion for 24 hr. Spectra were recorded in 50 mM DMPO with a microwave frequency of 9.77 GHz, 20 mW of microwave power, and a 0.5-G modulation amplitude. While no signal was observed in control cells, prominent DMPO-OH signals, 1:2:2:1 quartet with $a_H = a_N = 14.9$ G, were seen in cells activated with 1 μM A23187 that were blocked or quenched by either 1 mM L-NAME or SOD at 200 units/ml.

volume ratio of 7:1:1:1. Reversed-phase HPLC amino acid separation was performed using a Waters Pico-Tag column and the amino acid peaks from the samples were identified and quantitated by comparing with those from a standard (Pierce) containing each amino acid at 2 μmol/ml (14).

EPR Spectroscopy and Spin Trapping. Spin-trapping measurements of oxygen radical generation were performed on 5 × 10^6 cells per ml in PBS with DMPO at a final concentration of 50 mM (15, 16). The Fe^{2+} complex of MGD [Fe^{2+}–MGD_2 (Fe–MGD)] was used to trap NO formation from the cells (17, 18). Fresh stock solutions of Fe–MGD, 1:5, were prepared by adding ferrous ammonium sulfate to aqueous solutions of MGD. The final concentration used was 1 mM Fe^{2+}. EPR spectra were recorded in a quartz flat cell at room temperature with a Bruker ER 300 spectrometer operating at X-band with a 100-kHz modulation frequency and a TM 110 cavity, as described (15, 16). The microwave frequency and magnetic field were precisely measured using an EIP 575 frequency counter and Bruker ER 035 NMR gauss meter. Relative quantitation of the free radical signals was performed by double integration.

Immunocytochemistry and Measurement of Cellular Injury. Cells were plated on four-well Lab-Tek chamber slides (Nunc) that were coated with 1% gelatin and subjected to L-Arg depletion or normal control culture. After exposure to 1 μM A23187 for 18 hr, cells were fixed with 4% paraformaldehyde in PBS at room temperature for 30 min. After rinsing, the slides were incubated with affinity-purified mouse monoclonal anti-nitrotyrosine IgG (1:500 dilution, Upstate Biotechnology, Lake Placid, NY) (19, 20). The immunostaining was accomplished with an Extravidin peroxidase staining kit (Sigma) using 3-amino-9-ethylcarbazole as a chromogen.

For cytotoxicity assays, cells were grown in 24-well plates and exposed to normal control culture or L-Arg depletion. These cells were then incubated in Earle's balanced salt solution (EBSS) without phenol red (GIBCO/BRL) in the presence of A23187 (1 μM) for 18 hr. The lactate dehydrogenase (LDH) activity released in EBSS was determined with Sigma diagnostics LDH-optimized reagents (21).

Statistical Analysis. Results are expressed as the mean ± SEM. Student's unpaired *t*-test was used to determine the statistical significance of differences between the means, and a *P* value of <0.05 was considered significant.

RESULTS

Since purified nNOS has been reported to generate $^{\cdot}O_2^-$ at low concentrations of L-Arg (12), experiments were performed on nNOS-transfected 293 cells to determine whether depleting cytosolic L-Arg could trigger nNOS to produce $^{\cdot}O_2^-$. To deplete intracellular L-Arg, cells were incubated in L-Arg-free medium for various periods of time and then HPLC analysis was performed to measure cytosolic free L-Arg content. L-Arg free incubation substantially depleted cytosolic L-Arg. After L-Arg-free incubation for 8, 24, or 48 hr, cytosolic L-Arg concentrations were decreased from 35.2 ± 2.5 pmol per 10^6 cells (control) to 17.5 ± 1.8, 7.9 ± 0.9 or 15.8 ± 1.6 pmol per 10^6 cells, respectively ($P < 0.05$ versus control). The cells exposed to L-Arg-free incubation for 24 hr displayed the lowest cytosolic free L-Arg content.

EPR measurements of NO generation in the NOS-transfected 293 cells employed the NO trap Fe–MGD (18, 22). While no signals were observed in control unstimulated cells, stimulation with the Ca^{2+} ionophore A23187 (1 μM) triggered the generation of a prominent triplet spectrum with a central *g* value of 2.04 and hyperfine splitting of 12.7 G, characteristic of NO bound to Fe–MGD (Fig. 1 *Left*) (23, 24). These NO–Fe–MGD signals were completely blocked by the specific NOS inhibitor, L-NAME (1 mM), which confirmed that trapped NO was generated by NOS. In control experiments using the noninhibitory enantiomer D-NAME (1 mM), no decrease in the NO signal occurred, confirming that the inhibition seen with L-NAME was specifically due to blockade of NOS.

To investigate whether NOS produced $^{\cdot}O_2^-$ in L-Arg-depleted cells, 50 mM DMPO was used to trap oxygen free radicals formed by the cells preincubated in L-Arg-free medium for 24 hr. Although no signals were observed in unstimulated cells (Fig. 1 *Right*), a prominent signal appeared after activation with 1 μM A23187. The spectrum observed is a 1:2:2:1 quartet with $a_H = a_N = 14.9$ G, indicative of DMPO-OH (15, 16). These DMPO-OH signals were totally blocked by SOD (200 units/ml) but not affected by catalase (300 units/ml), suggesting that the observed signal was derived from $^{\cdot}O_2^-$. Blockade of NOS with 1 mM L-NAME resulted in a more than 90% decrease in the DMPO-OH signal. In control experiments performed using D-NAME (1 mM), no significant decrease was seen. Thus, $^{\cdot}O_2^-$ generated in L-Arg-depleted cells was derived from NOS.

To determine the role of cytosolic L-Arg concentrations in controlling NOS-mediated $^{\cdot}O_2^-$ generation in these cells, we examined the relationship of NO and $^{\cdot}O_2^-$ production to cytosolic L-Arg levels. In normal cultured cells in the presence of Fe–MGD, we observed maximum triplet NO signals but no DMPO-OH signals. When cytosolic L-Arg was depleted, NO production from these cells markedly decreased in proportion to the depletion of L-Arg (Fig. 2 *Left*). In contrast, $^{\cdot}O_2^-$ generation, monitored by the observed DMPO-OH signal, increased paralleling the decrease of cytosolic L-Arg concentrations (Fig. 2 *Right*). Maximum $^{\cdot}O_2^-$ formation was observed in the cells after a 24-hr L-Arg-free incubation, associated with the lowest cytosolic concentration of L-Arg. Thus, intracellular L-Arg depletion is required for NOS-catalyzed $^{\cdot}O_2^-$ generation in these cells. In four series of experiments, similar alterations in NO and $^{\cdot}O_2^-$ formation were observed in L-Arg-depleted cells (Table 1), establishing that cytosolic L-Arg concentration regulates the relative formation of NO or $^{\cdot}O_2^-$ from NOS.

NO reacts with $^{\cdot}O_2^-$ to form $ONOO^-$, a potent oxidant and mediator of cellular injury (25, 26). $ONOO^-$ reacts with tyrosine residues on proteins and yields a specific nitration product, nitrotyrosine, which presumably reflects the presence of $ONOO^-$ (19, 20). To determine whether NOS-mediated NO and $^{\cdot}O_2^-$ react to form $ONOO^-$ in L-Arg-depleted cells, we monitored nitrotyrosine by immunocytochemistry. Activation of NOS with A23187 resulted in prominent nitrotyrosine staining in L-Arg-depleted cells but not in control cells (Fig. 3 *A* and *B*). This staining was abolished by treatment with 1 mM L-NAME. Staining was also totally blocked by addition of excess nitrotyrosine (1 mM), confirming the specificity of antibody binding (Fig. 3*C*).

To assess whether NOS-mediated $ONOO^-$ generation caused cellular injury, we monitored cytotoxicity by measuring LDH release. With cells cultured in normal medium, LDH release was the same in the absence or presence of 1 μM A23187 (activities were 14.1 ± 2.0 and 15.8 ± 1.6 units/liter, P = not significant). Incubation in L-Arg-free medium also did not affect cell viability. However, in L-Arg-depleted cells, stimulation with A23187 increased LDH release 5-fold (from 14.1 ± 2.0 to 71.8 ± 4.8 units/liter; $n = 8$; $P < 0.01$) (Fig. 4). This increased LDH release could be largely prevented by the pretreatment with SOD (200 units/ml) or L-NAME (1 mM) with values of 28.2 ± 3.6 and 30.6 ± 3.5 units/liter, respectively ($P < 0.05$ versus L-Arg-depleted cells in the presence of A23187), confirming that these cytotoxic effects were elicited by the NO and $^{\cdot}O_2^-$ derived from activated NOS. In similar experiments performed using D-NAME (1 mM), no significant decrease in LDH release occurred with values of 60.6 ± 4.7 units/liter. Therefore, in L-Arg-depleted cells NOS generated both NO and $^{\cdot}O_2^-$ that reacted to form $ONOO^-$, which in turn resulted in cellular injury.

DISCUSSION

Recent studies have suggested that nNOS in the absence of L-Arg can generate reduced oxygen species including $^{\cdot}O_2^-$ and H_2O_2 (10–12). All prior evidence of NOS-mediated $^{\cdot}O_2^-$ generation, however, was based on studies of the isolated enzyme in which $^{\cdot}O_2^-$ generation might stem from alterations in the properties or conformation of the enzyme after isolation. Even more fundamental questions remained regarding the presence and biological relevance of this phenomena in intact cells.

Recently, direct methods have been developed enabling real time measurement of NO generation in biological cells and

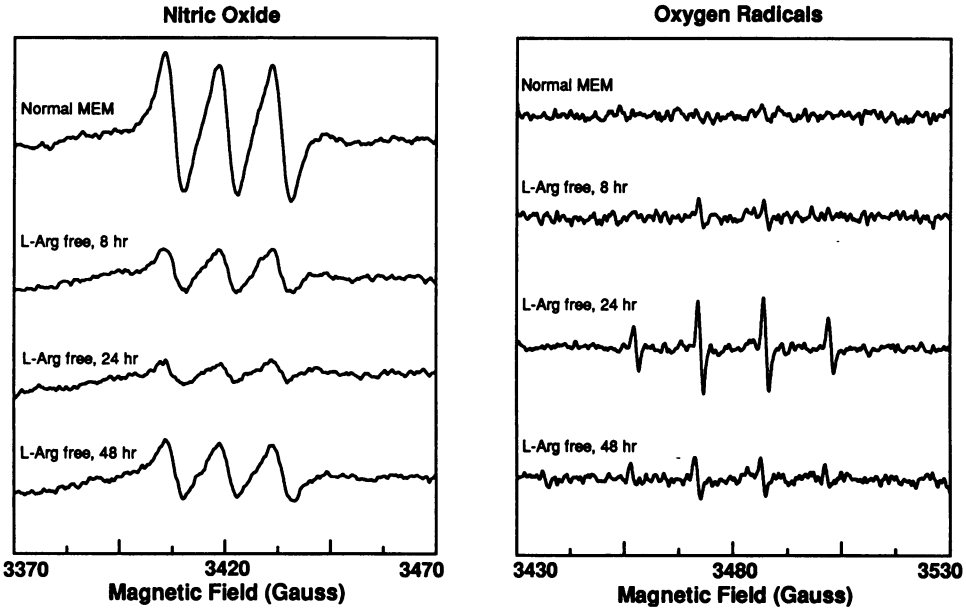

FIG. 2. NO decrease and oxygen radical increase in L-Arg-depleted cells. (*Left*) EPR spectra of NO generation from the NOS-transfected 293 cells subjected to different durations of L-Arg depletion. The spectra shown are from cells cultured in normal MEM or L-Arg-free medium for 8 hr, 24 hr, and 48 hr. (*Right*) EPR spectra measuring oxygen free radical generation from the NOS-transfected 293 cells after cytosolic L-Arg depletion. The spectra shown were from cell preparations incubated in normal MEM or L-Arg-free medium for 8 hr, 24 hr, or 48 hr. Spectra were recorded on 5×10^6 cells per ml in the presence of 1 μM A23187 as described in Fig. 1.

Table 1. Correlation of L-Arg depletion with NO and oxygen radical generation

	Control	L-Arg depletion		
		8 hr	24 hr	48 hr
L-Arg, pmol per 10^6 cells	35.2 ± 2.5	17.5 ± 1.8	7.9 ± 0.9	15.8 ± 1.6
NO, AU	17.2 ± 0.7	5.7 ± 0.5	3.1 ± 0.2	7.3 ± 0.3
Oxygen radicals, AU	0.2 ± 0.1	2.5 ± 0.3	12.4 ± 1.1	3.2 ± 0.4

L-Arg was measured by HPLC, NO was measured by EPR trapping with Fe–MGD, and oxygen radicals were measured by EPR trapping with DMPO. AU, arbitrary unit(s).

tissues (17, 18, 22, 27). Since NO is paramagnetic and reacts to form high-affinity nitroso complexes with a variety of metal complexes, the distinctive EPR spectra of these nitroso complexes permit quantitative measurements of NO generation (23). Fe–MGD is an ideal transition metal complex for trapping and measuring NO in tissues and *in vivo* in animals (18, 22, 24). The NO–Fe–MGD complex exhibits a characteristic triplet EPR spectrum, with a nitrogen hyperfine coupling constant a_N = 12.7 G, due to the coupling of the unpaired electron to the nitrogen nucleus of NO. Over the last decade EPR spin-trapping measurements have been widely applied to measure the generation of oxygen free radicals in biological systems. The spin trap DMPO, in particular, is a powerful and sensitive method for the detection of both extrinsic and intrinsic $^{\cdot}O_2^-$ generation from a variety of cells (15, 16, 28, 29). In the present study, we used both of these types of spin traps to enable direct unambiguous measurement of both NO and $^{\cdot}O_2^-$.

NO and $^{\cdot}O_2^-$ generation was measured in cells that were stably transfected to contain high expression of nNOS. In control cells no NO triplet signals were seen; however, after stimulation with the calcium ionophore A23187, large triplet signals were observed. The initiation of NO generation in these cells was, thus, dependent on the elevation of intracellular Ca^{2+} concentrations triggered by A23187. This Ca^{2+} dependence is a typical characteristic of nNOS (9). The observed NO generation in these stimulated cells was blocked by the specific NOS inhibitor L-NAME but not by the control compound D-NAME, confirming that NO was derived from NOS.

While no oxygen radical production was observed in control cells either in the presence or absence of A23187, when cells were depleted of L-Arg, prominent 1:2:2:1 quartet signals of DMPO-OH were seen. The DMPO-OH signal observed was completely quenched by SOD but not affected by catalase, indicating that this signal was derived from trapping of $^{\cdot}O_2^-$. The DMPO-OOH adduct can rapidly break down to form DMPO-OH. While this process can occur in simple chemical solutions, it may be further catalyzed by cellular peroxidases (30). The initiation of $^{\cdot}O_2^-$ generation by the cells also required elevation of intracellular Ca^{2+} concentration, as triggered by A23187, in a manner similar to that seen for NO. The observed $^{\cdot}O_2^-$ generation also was quenched more than 90% by the NOS blocker L-NAME but not by D-NAME.

The magnitude of intracellular L-Arg depletion is a crucial factor in switching NOS from the production of NO to $^{\cdot}O_2^-$. In control cells, where intracellular L-Arg was saturating, only NO formation was seen with no detectable $^{\cdot}O_2^-$. When cytosolic L-Arg was depleted, however, this triggered NOS-mediated $^{\cdot}O_2^-$ generation that increased as cytosolic L-Arg decreased. Conversely, NO production in these cells declined with L-Arg depletion. These observations fit with the detection of H_2O_2 formation as the L-Arg concentration is decreased to less than 100 μM (11). Based on an estimated cell volume of 0.5 pl (31), we calculate that the free L-Arg concentration in the cells decreased from 70.4 to 15.8 μM after 24 hr of incubation in the absence of L-Arg. With this decrease, a more than 20-fold increase in $^{\cdot}O_2^-$ generation and a more than 4- fold decrease in NO formation were observed. These changes parallel those reported with *in vitro* measurements of isolated NOS (11).

Impaired NO synthesis occurs in atherosclerosis, diabetes, and hypertension (32), and excessive production of NO is associated with cell and tissue damage, neurotoxicity, inflammation, reperfusion injury, and septic shock (33, 34). While NO in high concentrations can exert toxicity by direct binding to a variety of heme centers including the mitochondrial electron transport proteins (35), in biological systems NO may cause toxicity mainly through the diffusion-limited reaction of NO with $^{\cdot}O_2^-$ to generate $ONOO^-$ (25, 26). $ONOO^-$ is a highly reactive oxidant that causes lipid peroxidation, thiol oxidation, and nitrosation or nitration of the functional groups of several amino acids including tyrosine. In L-Arg-depleted cells, we observed that NOS catalyzed both NO and $^{\cdot}O_2^-$ synthesis, suggesting that NO and $^{\cdot}O_2^-$ react to form $ONOO^-$, which in turn causes amino acid nitration and cellular injury. Nitrotyrosine formation was observed in L-Arg-depleted cells after activation and this process was blocked by inhibition of NOS. Furthermore, activation of NOS caused cytotoxicity in these cells with marked LDH release that was inhibited by the NOS blocker L-NAME or the $^{\cdot}O_2^-$ dismutating enzyme SOD.

Our findings may be relevant to the pathogenesis of cell and tissue injury in disease states such as ischemia and wound healing where a lack of perfusion could lead to tissue L-Arg depletion (36) and $ONOO^-$ formation. It was previously assumed that $ONOO^-$ is formed when NO generated from NOS reacts with exogenous $^{\cdot}O_2^-$, whereas our findings show

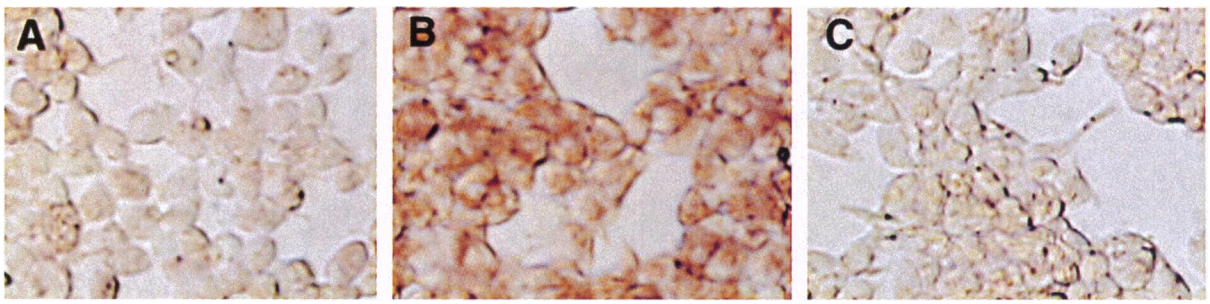

FIG. 3. Immunocytochemical detection of nitrotyrosine formation. After exposure to 1 μM A23187 for 18 hr, cells were incubated with the anti-nitrotyrosine monoclonal antibody and immunostaining was performed by Extravidin peroxidase. Prominent immunostaining of nitrotyrosine was observed in L-Arg-depleted cells (*B*) but not in cells cultured in normal MEM (*A*). This staining was totally blocked by preincubation of the primary antibody with 1 mM nitrotyrosine (*C*).

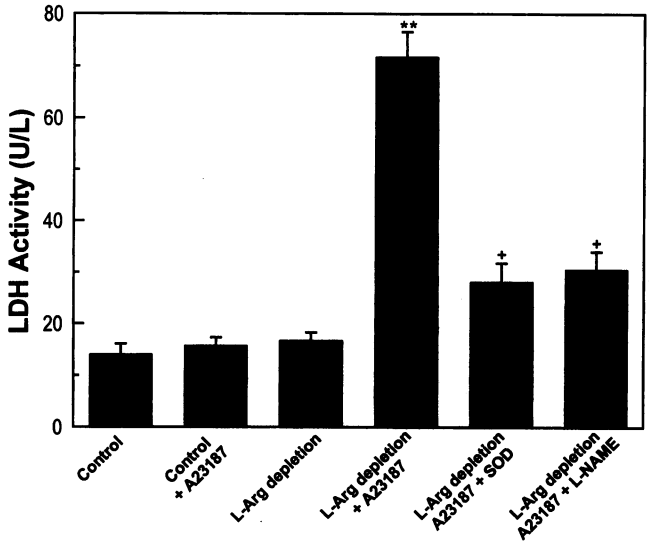

FIG. 4. Measurement of NO- and $^{\cdot}O_2^-$-mediated cellular injury in L-Arg-depleted and control cells. Cell injury was assessed by measuring LDH release from cells incubated for 18 hr in the presence or absence of 1 μM A32187. Experiments were also performed in the presence or absence of L-NAME at 1 mM or SOD at 200 units/ml. Activating NOS in L-Arg-depleted cells caused marked LDH release and this effect was largely prevented by the prior administration of L-NAME or SOD. Data were expressed as the mean ± SEM obtained from eight experiments (**, $P < 0.01$ versus control; +, $P < 0.05$ versus L-Arg-depleted cells in the presence of A23187).

that cellular NOS itself generates $^{\cdot}O_2^-$ with secondary formation of $ONOO^-$ leading to cellular injury or death.

This work was supported by National Institutes of Health Grants HL-38324 and HL-52315, and an American Heart Association Established Investigator Award to J.L.Z. V.L.D. is supported by U.S. Public Health Service (USPHS) Grant NS-33142, the American Heart Association, and the Alzheimer's Association. T.M.D. is supported by USPHS Grants NS-01578 and NS-33277, the International Life Sciences Institute, and a Paul Beesons Physicians Scholar Award in Aging Research. S.H.S. is supported by USPHS Grant DA-00266 and Research Scientist Award DA-00074.

1. Moncada, S., Palmer, R. M. & Higgs, E. A. (1991) *Pharmacol. Rev.* **43,** 109–142.
2. Ignarro, L. J. (1990) *Annu. Rev. Toxicol.* **30,** 535–560.
3. Lowenstein, C. & Snyder, S. H. (1992) *Cell* **70,** 705–707.
4. Nathan, C. & Xie, Q.-w. (1994) *J. Biol. Chem.* **269,** 13725–13728.
5. Nathan, C. & Xie, Q.-w. (1994) *Cell* **78,** 915–918.
6. Marletta, M. A. (1994) *Cell* **78,** 927–930.
7. Bredt, D. S., Hwang, P. M., Glatt, C. E., Lowenstein, C., Reed, R. R. & Snyder, S. H. (1991) *Nature (London)* **351,** 714–718.
8. Marletta, M. A., Yoon, P. S., Iyengar, R., Leaf, C. D. & Wishonk, J. S. (1988) *Biochemistry* **27,** 8706–8711.
9. Griffith, O. W. & Stuehr, D. J. (1995) *Annu. Rev. Physiol.* **57,** 707–736.
10. Mayer, B., John, M., Heinzel, B., Werner, E. R., Wachter, H., Schultz, G. & Bohme, E. (1991) *FEBS Lett.* **288,** 187–191.
11. Heinzel, B., John, M., Klatt, P., Bohme, E. & Mayer, B. (1992) *Biochem. J.* **281,** 627–630.
12. Pou, S., Pou, W. S., Bredt, D. S., Snyder, S. H. & Rosen, G. M. (1992) *J. Biol. Chem.* **267,** 24173–24176.
13. Shinobu, L. A., Jones, S. G. & Jones, M. M. (1984) *Acta Pharmacol. Toxicol.* **54,** 189–194.
14. Deyl, Z., Hyanek, J. & Horakova, M. (1986) *J. Chromatogr.* **379,** 177–250.
15. Zweier, J. L., Kuppusamy, P. & Lutty, G. A. (1988) *Proc. Natl. Acad. Sci. USA* **85,** 4046–4050.
16. Zweier, J. L., Broderick, R., Kuppusamy, P., Thompson-Gorman, S. L. & Lutty, G. A. (1994) *J. Biol. Chem.* **269,** 24156–24162.
17. Lai, C. S. & Komarov, A. M. (1994) *FEBS Lett.* **345,** 120–124.
18. Zweier, J. L., Wang, P. & Kuppusamy, P. (1995) *J. Biol. Chem.* **270,** 304–307.
19. Beckman, J. S., Ye, Y. Z., Anderson, P. G., Chen, J., Accavetti, M. A., Tarpey, M. M. & White, C. R. (1994) *Biol. Chem. Hoppe-Seyler* **375,** 81–88.
20. Haddad, I. Y., Pataki, G., Hu, P., Galliani, C., Beckman, J. S. & Matalon, S. (1994) *J. Clin. Invest.* **94,** 2407–2413.
21. Lipton, S. A., Choi, Y. B., Pan, Z. H., Lei, S., Chen, H. S. V., Sucher, N. J., Loscalzo, J., Singel, D. J. & Stamler, J. S. (1993) *Nature (London)* **364,** 626–632.
22. Zweier, J. L., Wang, P., Samouilov, A. & Kuppusamy, P. (1995) *Nat. Med.* **1,** 804–809.
23. Lancaster, J. R., Jr., Langehr, J. M., Bergonia, H. A., Murase, N., Simmons, R. L. & Hoffman, R. A. (1992) *J. Biol. Chem.* **267,** 10994–10998.
24. Komarov, A., Mattson, D., Jones, M. M., Singh, P. K. & Lai, C. S. (1993) *Biochem. Biophys. Res. Commun.* **195,** 1191–1198.
25. Beckman, J. S., Beckman, T. W., Chen, J., Marshall, P. A. & Freeman, B. A. (1990) *Proc. Natl. Acad. Sci. USA* **87,** 1620–1624.
26. Radi, R., Beckman, J. S., Bush, K. M. & Freeman, B. A. (1991) *J. Biol. Chem.* **266,** 4244–4250.
27. Kubrina, L. N., Caldwell, W. S., Mordvintcev, P. I., Malenkova, I. V. & Vanin, A. F. (1992) *Biochim. Biophys. Acta* **1099,** 233–237.
28. Rosen, H. & Klebanoff, S. J. (1979) *J. Clin. Invest.* **64,** 1725–1729.
29. Rosen, G. M. & Freeman, B. A. (1984) *Proc. Natl. Acad. Sci. USA* **81,** 7269–7273.
30. Finkelstein, E., Rosen, G. M. & Rauckman, E. J. (1982) *Mol. Pharmacol.* **21,** 262–265.
31. Hecker, M., Sessa, W. C. Harris, H. J., Anggard, E. E. & Vane, J. R. (1990) *Proc. Natl. Acad. Sci. USA* **87,** 8612–8616.
32. Moncada, S. & Higgs, E. A. (1993) *N. Engl. J. Med.* **329,** 2002–2012.
33. Gross, S. S. & Wolin, M. S. (1995) *Annu. Rev. Physiol.* **57,** 737–769.
34. Dawson, V. L., Dawson, T. M., London, E. D., Bredt, D. S. & Snyder, S. H. (1991) *Proc. Natl. Acad. Sci. USA* **88,** 6368–6371.
35. Nathan, C. F. & Hibbs, J. B., Jr. (1991) *Curr. Opin. Immunol.* **3,** 65–70.
36. Albina, J. E., Mills, C. D., Barbul, A., Thirkill, C. E., Henry, W. L., Jr., Mastrofrancesco, B. & Caldwell, M. D. (1988) *Am. J. Physiol.* **254,** E459–E467.